2022

Understanding Surface Water--Groundwater Connectivity and Discharge in Arctic Deltas

Lindsey N. Aman
West Virginia University, lna00002@mix.wvu.edu

Understanding Surface Water—Groundwater Connectivity and Discharge in Arctic Deltas

Lindsey Aman Cromwell

Thesis submitted to the Eberly College of Arts and Sciences at West Virginia University

in partial fulfillment of the requirement for the degree of

Master of Science in

Geology

Christopher J. Russoniello, Ph.D., Chair

Charles Shobe, Ph.D.

Deon Knights, Ph.D.

Department of Geology and Geography

Morgantown, West Virginia

2022

Keywords: Arctic, Talik, Surface Water—Groundwater Connectivity, Groundwater Discharge

Abstract

Understanding Surface Water Groundwater—Groundwater Connectivity and Discharge in Arctic Deltas

Lindsey Aman Cromwell

Increased warming is driving unprecedented hydrologic changes within arctic deltas with implications for water storage, solute processing, and terrestrial and marine ecology. Thermokarst lakes within Arctic deltas store flood waters and filter solutes and sediments, thus moderating the impact of flood water discharge to arctic seas. However, this moderating influence is diminishing as lakes shrink on annual and seasonal time scales, especially close to active channels where lakes are shrinking most rapidly. This study investigates surface water-groundwater connectivity in arctic delta plains with coupled flow and heat transport models to provide a mechanistic understanding of how lake-channel proximity will impact aquifer connectivity and associated groundwater discharge to downgradient channels. Results show near-channel lakes have increased lake-to-channel advective heat transport and perennial connectivity and discharge to downgradient channel. However, connectivity and discharge from far-channel lakes is seasonal, where near-zero discharge occurs when lake and channel taliks are isolated. Near-channel lakes are perennially draining through taliks contributing to observed increases in Arctic channel baseflow. Lake drainage highlights the importance that lakes – especially near-channel lakes most vulnerable to loss – will have changing roles in moderating flood waters and nutrient processing before discharging to the arctic seas.

Table of Contents

Acknowledgements

I would like to begin by thanking my advisor, Dr. Chris Russoniello, for being a supportive mentor throughout my experience as a graduate student at West Virginia University. Chris has the ability to make research an enjoyable experience, even when it's not, and has pushed me to the best possible researcher, writer, teacher, and mentor. I will always be grateful for the opportunity to study Arctic hydrogeology, a path that was outside of my comfort zone, but has made me the student I am today. I would also like to thank my additional committee members Dr. Charlie Shobe and Dr. Deon Knights along with Chris for always having an open door to answer my *many* questions, research and otherwise.

Even as modeling problems seemed to be at every turn, I always seemed to have a resource at my side. For this, I would like to thank Dr. Carlos Andres Rivera Villarreyes, Dr. Anner Paldor, and Dr. James Heiss for their guidance and assistance with unfamiliar software.

Finally, I would like to thank my friends and family that have supported me through this journey. To my parents, Heidi and Terry, thank you for never doubting me even when I changed my major 3 times as an undergrad before finding Geology, and for supporting me in my research goals when that new major allowed me to work from Taiwan to the Arctic Circle. To my husband Copeland, thank you for supporting and still tolerating me through our mutual stress of graduate school, and for teaching me Python when StackOverflow failed me. To my friends and lab partners past and present, your friendships and words of encouragement will reach well beyond the country roads that led me home.

This research would not have been possible without the support of the West Virginia University Geology and Geography Department, the WVU Carl del Signore Scholarship, and the Geological Society of America Graduate Student Research Grant.

Chapter 1: Introduction

Arctic delta environments are crucial to the regulation of nutrient distribution, temperature, and salinity into the Arctic Ocean (Aagaard et al., 1989; ACIA 2004; Holland et al., 2007; Holmes et al., 2001). Riverine input to the Arctic Ocean is dominated by the deltas of six rivers—Lena, Mackenzie, Kolyma, Colville, Yenisey, and Yukon —which combined account for 2/3 of the total fresh discharge to the Arctic Ocean (Holmes et al., 2012). Within these deltas, hundreds of thousands of thermokarst lakes are present due to permafrost thaw and seasonal flood events (Piliouras and Rowland, 2019). These seasonal flood events, known as the spring freshet which accompany ice thaw and snow melt during the late spring or early summer, provide sudden fluxes of relatively warm water, solutes, and sediments into the delta system. Arctic thermokarst lakes serve as nutrient filtration centers and fine sediment traps for transient water storage before discharging to the ocean (Emmerton et al., 2007). For example, lakes in the Mackenzie Delta in NW Canada may hold up to 16% of total flood volume, and specifically 47% of the spring freshet (Piliouras and Rowland, 2019; Emmerton et al., 2007), while lakes in the Colville Delta may hold 5% of total flood volume (Piliouras and Rowland, 2019). Lakes can directly impact fluid, solute, and sediment potential residence times before discharging to the arctic seas.

Arctic lakes in discontinuous permafrost zones have been shrinking both seasonally and annually (Nitze et al., 2017; Jepsen et al., 2012), with lakes closer to active delta channels shrinking more than those more distant from the channels (Vulis et al., 2020). The declines in lake volumes and surface areas have implications for water storage, flood mitigation, sedimentation, and nutrient transport by decreasing fluid residence times within thermokarst lakes. Additionally, arctic river baseflows are increasing and have been correlated to potential

precipitation increase, increased permafrost thaw and hydrologic connectivity, and/or the decrease in lake storage (St. Jacques and Sauchyn, 2009). River baseflows may also be increasing due to the formation of taliks, which are unfrozen channels within permafrost that can connect between surface water bodies (Scheidegger and Bense, 2014). Taliks allow groundwater to flow from the lakes to downgradient rivers in permafrost settings where groundwater transport is generally restricted due to the presence of ice (Lamontagne-Halle et al., 2018). The correlation between increased river baseflows and lake shrinkage may be due to increased hydrogeologic connectivity within the permafrost increasing discharge from nearby lakes to downgradient channels.

Lake sill elevations and lake-channel proximity serve as the primary controls on river and lake surface water connectivity (Emmerton et al., 2007), however groundwater connectivity in arctic deltas remains poorly understood. Within the Mackenzie Delta, lake sill elevations can be classified with regards to closure, where closure describes the continuity of connectivity between the river channel and neighboring lakes. These classifications include no-closure (< 1.5 m ASL) in which lake-channel connectivity is persistent, low-closure (1.5 – 4 m ASL) in which lake-channel connectivity is common, and high-closure (> 4 m ASL) (Marsh and Hey, 1989) in which lake-channel connectivity is absent. Lake sill elevations correlate to the ease of lake inundation due to the spring freshet, where lakes with higher sill elevations are less likely to obtain relatively warmer temperature waters from the spring freshet. Increased distance from the river channel may decrease surface water connectivity as seasonal flooding occurs in the active delta channel (Piliouras and Rowland, 2019) and remain isolated. As most arctic lakes are within a few channel widths from the main channel (Piliouras and Rowland, 2019), it is useful to

understand this relationship on spatial and temporal scales and the subsequent effect on lake fluid and energy budgets.

Groundwater connectivity relies on the formation of taliks to create unfrozen pathways for flow in permafrost settings. Without taliks, frozen ground greatly inhibits groundwater flow by several orders of magnitude (Walvoord and Kurylyk, 2016). Lakes with greater surface water connectivity may also increase groundwater connectivity as the spring freshet floods adds an influx of relatively warm waters, increasing lake-bottom temperature. Lake bottom temperatures have a direct impact on inducing talik formation (Burn, 2002; Burn, 2003; Rowland et al., 2011). The continual increase in lake-bottom temperatures over time can induce a positive feedback loop promoting permafrost thaw, causing groundwater connectivity to increase. Thus, lakes with greater connectivity to the channel based on respective sill elevations, or lakes closer to active channels with increased groundwater heat transfer may experience greater sub-lacustrine permafrost thaw.

Permafrost affects surface water-groundwater dynamics in northern regions by acting as a low hydraulic conductivity (K) unit, inhibiting groundwater flow between supra-permafrost and sub-permafrost aquifers, surface water interactions, and other unfrozen areas (Walvoord and Kurylyk, 2016). The active layer of the aquifer, which lies above the permafrost table and undergoes annual freeze/thaw, is the greatest contributor to surface water – groundwater connectivity. The permafrost table has been noted to decrease below surface water bodies, as heat transfer from river and lake bottom temperatures thaw surrounding subsurface regions (Rowland et al., 2011). Unfrozen passages within the subsurface cause preferential flow of relatively warm groundwater to act as a positive feedback loop of continued permafrost melt through advective heat transfer (McKenzie and Voss, 2012). Thus, it is important to characterize

the mechanisms driving lake shrinkage, whether it is continued permafrost thaw through warm lake bottom temperatures, or increased connectivity driving increased discharge to downgradient delta channels. This study investigates the effect of lake-channel proximity and connectivity on seasonal discharge to downgradient arctic channels to bridge the gap between near-channel lake shrinkage and increases in channel baseflow.

Chapter 2: Field Work

Field measurements of surface water—groundwater interactions have been limited due to the remote nature of arctic deltas. There remains a great need for accurate, in-situ field data for arctic hydrogeologic modeling studies. Heat transfer is a primary tool for understanding surface water-groundwater interactions (Rau et al., 2014), as heat tracing methods can detect small fluxes (Kurylyk et al., 2019) and measurements are relatively inexpensive and easy to collect. To visualize the effect of surface water insulation on depth to permafrost, we collected an in-situ, 2-dimensional, cross-sectional temperature profile to place our model results in a real-world context.

Due to COVID-19 related travel restrictions, the temperature profile was collected in an Arctic stream south of Utqiagvik, Alaska to serve as a proxy to Arctic delta channel environments (Figure S6). Temperature-depth profiles were measured with 30 cm depth intervals using a ¼" x 153 cm temperature probe inserted into the ground until refusal – typically with an audible tap. We considered refusal depth to represent frozen aquifer top. The half-width cross section extended 30 m from the center of the stream to the edge of the stream valley, and lateral measurement density varied based on surface morphology (0.83 m - 15 m), with closer-spaced temperature-depth profiles near the channel for better temperature gradient resolution. Relative

ground elevation of each profile was surveyed with a handheld optical level and rod to assign vertical elevations.

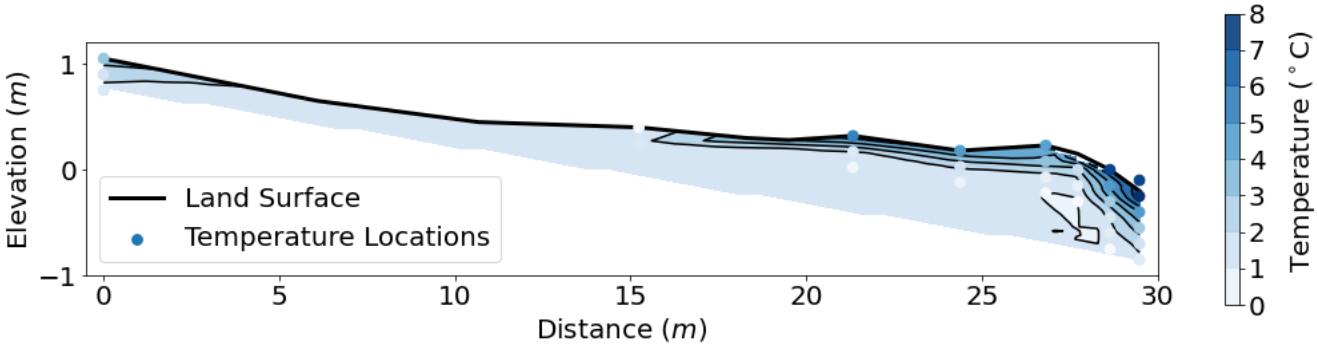

Figure 1. Cross-sectional temperature profile to visualize depth-to-permafrost surrounding surface water bodies in arctic landscapes. Colors represent temperatures in °C, while elevation represents relative elevation from the surface of the channel, and distance indicating distance from channel center. The land surface is denoted by the thick black line and temperature contours are denoted by thin black lines beneath the surface.

Surface water bodies act as insulation and thaw the surrounding permafrost creating a greater depth to permafrost seen in results from the temperature profile (Figure 1). At the middle of the stream channel, permafrost depth from the channel bed reaches a depth of 0.70 m while at an approximate distance of 15 m from the channel, depth to permafrost is approximately 0.15 m. As distance from the channel increases, depth to the permafrost decreases with decreasing surface water insulation.

Chapter 3: Understanding Surface Water—Groundwater Connectivity and Discharge in Arctic Deltas

3.1 Introduction

Arctic delta environments are increasingly stressed as the Arctic experiences temperatures rising at twice the global average (ACIA, 2004). Subsequent increased permafrost melt over longer warm seasons and precipitation is driving unprecedented hydrology changes. The Arctic Ocean receives 11% of the global river discharge, while only containing 1% of global ocean water by volume (Holmes et al., 2012) making it disproportionately sensitive to riverine input. Within the next century, projections indicate increased river discharge through arctic deltas will influence nutrient, temperature, and salinity inputs to the already vulnerable Arctic Ocean (ACIA, 2004). As annual river discharges increase, arctic communities and ecosystems will become increasingly susceptible to spring flood events during the spring freshet (Whalen et al., 2009) with implications for arctic infrastructure and ecosystem health (Jorgenson et al., 2009).

Arctic deltas contain hundreds of thousands of thermokarst lakes that can temporarily store spring floodwater to mitigate these flooding events (Piliouras and Rowland, 2020), but the quantity and capacity of these lakes remains poorly characterized and the expected change under future conditions is even less certain. Thermokarst lakes, which form by subsidence as relatively warm flood waters melt ice-rich permafrost, trap nutrients and fine sediments (Piliouras and Rowland, 2020). These lakes also temporarily store up to 16% of total spring freshet flood volume in thermokarst-rich regions such as the Mackenzie delta in Northwest Canada, which mitigates spring flooding effects by damping peak discharge (Piliouras and Rowland, 2020), increasing water residence times, and increasing solute processing potential (Emmerton et al., 2008). Recent remote sensing studies show thermokarst lakes in discontinuous permafrost zones

are shrinking on seasonal and annual time scales (Nitze et al., 2017; Jepsen et al., 2012), and shrinkage rates increase with proximity to active delta channels (Vulis et al., 2020). This decline in lake volume and surface area likely reduces flood storage capacity and has implications for variability of riverine discharge to the Arctic Ocean especially as channel-proximal lakes have greater capacity to store flood waters (Emmerton et al., 2007).

Lake shrinkage in Arctic deltas within discontinuous permafrost zones may be partially attributed to thawed permafrost, *taliks*, beneath these lakes, which allows lake water to drain through the aquifer (Lamontagne-Halle et al., 2016; Scheidegger and Bense, 2014). Taliks form as relatively warm surface water bodies transfer heat into, insulate, and thaw underlying and adjacent permafrost (Rowland, 2011; Mackenzie and Voss, 2013). *'Open taliks'* that form beneath perennially liquid surface water bodies and connect to other unfrozen areas increase surface water – groundwater connectivity (Burn, 2005; Walvoord and Kurylyk, 2016). Taliks drive positive feedback loops for melt wherein warm water flowing through a talik thaws additional permafrost, which increases the cross-sectional area allowing greater flow and heat transport (Rowland, 2011; Mackenzie and Voss, 2013). This enhances lake drainage through groundwater to downgradient channels (Dimova et al., 2015; Scheidegger and Bense, 2014; Lamontagne-Halle et al., 2016), which aligns with recent observations of decreased surface area and number of lakes (Nitze et al., 2017; Jepsen et al., 2012; Vulis et al., 2020), and increased winter baseflows of 5-25% in Mackenzie Delta channels (Yang et al., 2014).

While it is well documented that sub-lacustrine talik formation leads to increased discharge from lakes to near surface storage and flow (Arp et al., 2016; Scheidegger and Bense, 2014; Vulis et al., 2020; You et al., 2016), a mechanistic understanding of why near-channel lakes shrink more quickly than lakes more distant from channels is currently lacking. This study

applies fully coupled heat and fluid transport models with aquifer freeze-thaw capability to examine the effect of lake-channel proximity on aquifer connectivity and associated groundwater discharge to downgradient channels. Increased aquifer connectivity and groundwater discharge to downgradient channels may decrease lake fluid residence times, thus decreasing nutrient processing potential before discharging to the arctic seas causing implications for ecosystem health.

3.2 Methods

This study investigates how lake presence and proximity affect seasonal discharge to Arctic channels with 2-D cross-sectional, fully coupled, variably saturated fluid and heat transport models with aquifer freeze-thaw capability using Finite Element Subsurface FLOW system (FEFLOW) with the piFreeze plug-in (MIKE, 2016). PiFreeze simulates the effect of freezing by assigning temperature-dependent hydraulic conductivity (K) values representative of frozen ground to simulate the effect that permafrost/ice has on inhibiting subsurface flow (MIKE, 2016; Walvoord and Kurylyk, 2016). In all study simulations, aquifer regions greater than 1°C were considered fully thawed and assigned a saturated hydraulic conductivity (K) of 0.09 m/day. Aquifer regions less than -1°C were considered fully frozen and K was prescribed four orders of magnitude less than the saturated K. K decreased log-linearly in a mix between thawed and frozen (slushy) aquifer regions from 1°C to -1°C. Models were split between No Lake (1) and Lake (4) models.

3.2.1 No Lake

To understand discharge to downgradient stream channels in the absence of lakes, a base model (hereafter referred to as No Lake model) was constructed. This No Lake model generally

follows domain, parameterization, and boundaries of Lamontagne-Halle et al. (2016) to allow comparison with previous work results, but decreased domain thickness allowed higher resolution of surface processes. Models were constructed with two-dimensional, cross-sectional domains (w = 60 m, h = 51 m) with a 2% slope across the land surface (x = 0-50 m) and the rightmost 10 m representing a 5-m deep channel bank (Figure S1). Each model is homogeneous aside from a thin (0.5 m) channel bed confining layer ($K = 9\times10^{-4}$). Additional parameters controlling fluid and heat transport are listed in Supplemental Table S1.

Flow and temperature boundary conditions were defined along the land surface and channel bed. The land surface was assigned time-variant temperature and recharge boundaries to simulate seasonal forcing. A maximum hydraulic head constraint prevented recharge to cells with heads exceeding land surface elevation. Land surface temperature was applied as an annual sinusoidal air temperature (15°C amplitude; min and max temperatures in late January and late July, respectively) representative of Utqiagvik, AK (NCEI, 2022). Time-varying recharge (0.2 m/yr average) was prescribed as follows: a 36-day pulse of recharge (up to 0.003 m/d) representing spring snow and channel ice melt, hereafter *freshet*, was applied starting 15 days after mean daily temperatures exceed 0°C; 0.0013 m/d during the warm season; and a brief 8.1e-5 m/d during the start of the cold season (Figure 2; Lamontagne-Halle et al., 2016). Recharge was prescribed as zero when land surface temperatures were below 0°C to represent surface snow accumulation. The channel bed was assigned a constant head boundary (48 m) and a seasonally varying temperature based on measured Arctic stream bottom temperatures (Burn, 2003). A drain was prescribed in channel-slope cells above the channel water level to allow a subaerial groundwater seepage face. Insulation at the land surface (e.g from accumulated snow and vegetation) was not

considered (e.g. Schneidegger and Bense, 2014). A geothermal heat flux of 0.085 W/m was prescribed to the domain base (Lamontagne-Halle et al., 2016).

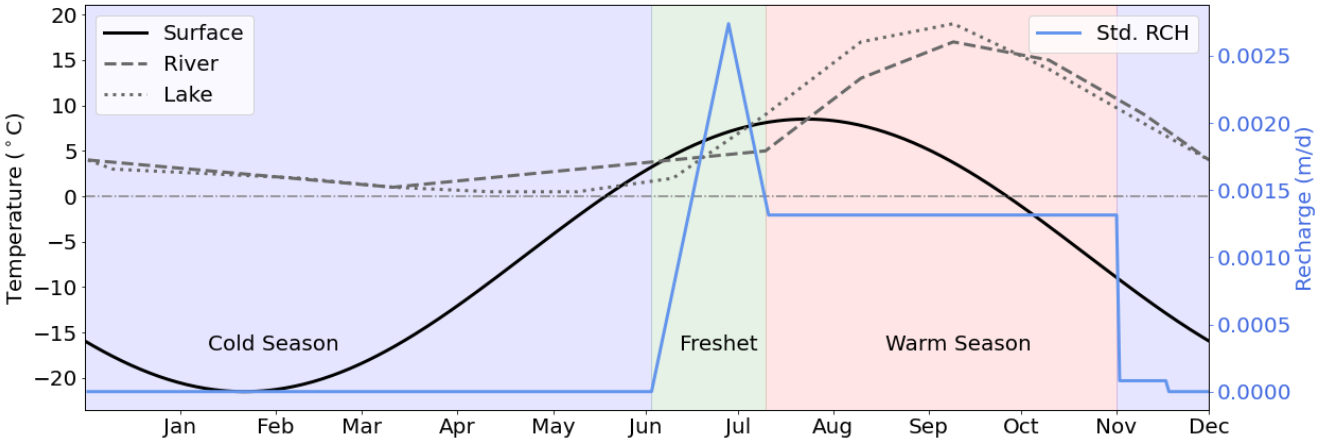

Figure 2. Boundary conditions for domain surface (Surface Temperature and Recharge) for 1 annual cycle. Temperatures measured at channel and lake-bottom (Burn, 2003). Std. RCH represents the standard average recharge of 0.2 m/yr used for all models.

All models were run in 2 phases. Phase 1 was a 30,000-year transient simulation with constant -6.5°C temperature condition at the surface and the constant geothermal heat flux applied to the bottom of the domain to establish permafrost distribution (Lamontagne-Halle et al., 2016). Phase 1 results were applied as Phase 2 initial conditions. Phase 2 were transient simulations with seasonally variant boundary conditions. To understand channel discharge from Phase 2 model results, analysis was conducted at year 30 as remote-sensing studies view annual thermokarst lake change in 30-year intervals (Nitze et al., 2017; Jepsen et al., 2012). Temperature and fluid data were extracted from FEFLOW and analyzed in Python. Channel discharge values were reported as a linear flux from aquifer discharge to the channel, where this flux occurs along the 6.3 m inundated channel bank.

3.2.2 Lake Models

Four *Lake* models were simulated with the same domain geometry and boundary conditions as the No Lake model, but with a 5 m wide, 1.37 m deep lake added with a right edge at either 5, 10, 20, or 40 meters from the channel slope (Figure S2) – hereafter referred to as *5 m Lake*, *10 m Lake*, *20 m Lake*, and *40 m Lake*, respectively. Each lake was simulated with a constant head boundary equal to the lake surface elevation (equal to surface elevation if lake did not exist). Lakes were assigned this size as they have been shown to have unfrozen lake bottoms throughout winter months (Emmerton et al., 2007). Time variant lake bottom temperatures were assigned from measured arctic lake bottom temperatures (Burn, 2003).

3.2.3 Sensitivity Analyses

To understand how the seasonal temperature amplitude, hydraulic conductivity, and recharge affect annual and seasonal groundwater discharge to the channel, sensitivity analyses were conducted. Seasonal temperatures and recharges were applied as annual cyclic functions, where temperature amplitude and mean annual recharge were adjusted (Figure S3; Table S2). All simulations were performed as No Lake models as the No Lake model was the control for comparison in Lake models, with adjusted values in Phase 1 and Phase 2 scenarios with the same final simulation times. Darcy flux at channel nodes and temperatures for the entire domain were extracted post-simulation and compared to No Lake results.

3.3 Results and Discussion

3.3.1 No Lake

Perennial below-channel taliks form within the No Lake simulation, but the remainder of the aquifer is seasonally or perennially frozen (Figure 3D), which restricts aquifer transmissivity

and groundwater discharge to the channel. *Active zones* which freeze and thaw annually are restricted to the top 2m of the aquifer, adjacent to the channel talik, and along the channel slope. The channel slope active zone enables the necessary connection for surface recharge to flow and discharge to the perennially unfrozen channel talik. Prescribed above-freezing channel bottom temperatures maintain the perennially persistent channel talik, but reduced transmissivity in the frozen aquifer greatly restricts flux from early November to mid-May (Figure 4A). Freely available water within the channel talik is confined to only below the channel during these conditions, which causes near-zero discharge. Recharge to the talik from the channel occurs due to low head as the talik refreezes (Figure 4B).

The aquifer warms and thaws from top down during spring, and the unfrozen aquifer area increases as the thawed front propagates downward (Figure 3; Figure 4A). The spring freshet occurs soon after initial thaw, which was prescribed as high potential recharge. However, the aquifer quickly becomes saturated as the permafrost restricts discharge downgradient, so the maximum hydraulic head constraint prevents most potential recharge to enter (~80 % in the No Lake model), which may be considered surface runoff. As the aquifer warms and thawed area increases, increased transmissivity between the thawed surface-active layer and the channel yields increased discharge to the channel with peak discharge coincident with late July peak surface temperatures.

As surface temperatures begin to decline below freezing in late September, the surficial active layer refreezes from above, and aquifer transmissivity decreases as the frozen front propagates downwards (Figure 3). Discharge is increasingly restricted (Figure 4) until the surficial active layer fully freezes in December and restricts groundwater flow towards the channel talik.

Much of the No Lake model aquifer remains fully frozen throughout a 1-year cycle, and due to year-long unfrozen channel bottom temperatures, an isolated talik remains beneath the channel. As surface temperatures increase, an unfrozen zone propagates downward and increases connectivity between the surface and the channel. No Lake models show maximum channel discharge during times of maximum connectivity, slightly after peak surface temperatures, where recharge at the surface can discharge to the channel. As surface temperatures decrease, the unfrozen zone begins to refreeze from the top down, pinching out the unfrozen zone and decreasing connectivity and channel discharge.

3.3.2 Lake Models

Lake models with 10, 20, and 40 m lake-channel distance had seasonally frozen active zones that greatly reduced groundwater flow during winter compared to the 5 m Lake model that developed a perennial lake-channel talik that allowed perennial groundwater flow and channel discharge (Figure 3). Isolated, sub-lake taliks were perennially persistent in 10, 20, and 40 m lake simulations, but these were disconnected from the channel talik during the cold season (Figure 3D). Lake-channel connectivity developed during the warm season as the active layer thawed and transmitted flow from the lake to the channel. A perennial lake-channel talik in the 5 m Lake simulation maintained a cold season lake-channel connection (Figure 3D) and cold season discharge to the channel (Figure 4B). The 10 m, 20 m, and 40 m lake models had near-zero cold season discharge. Lake-channel proximity in the 10 m Lake model lengthened the duration of lake-channel connectivity enabling a longer period of seasonal lake discharge compared with 20 and 40 m Lake models.

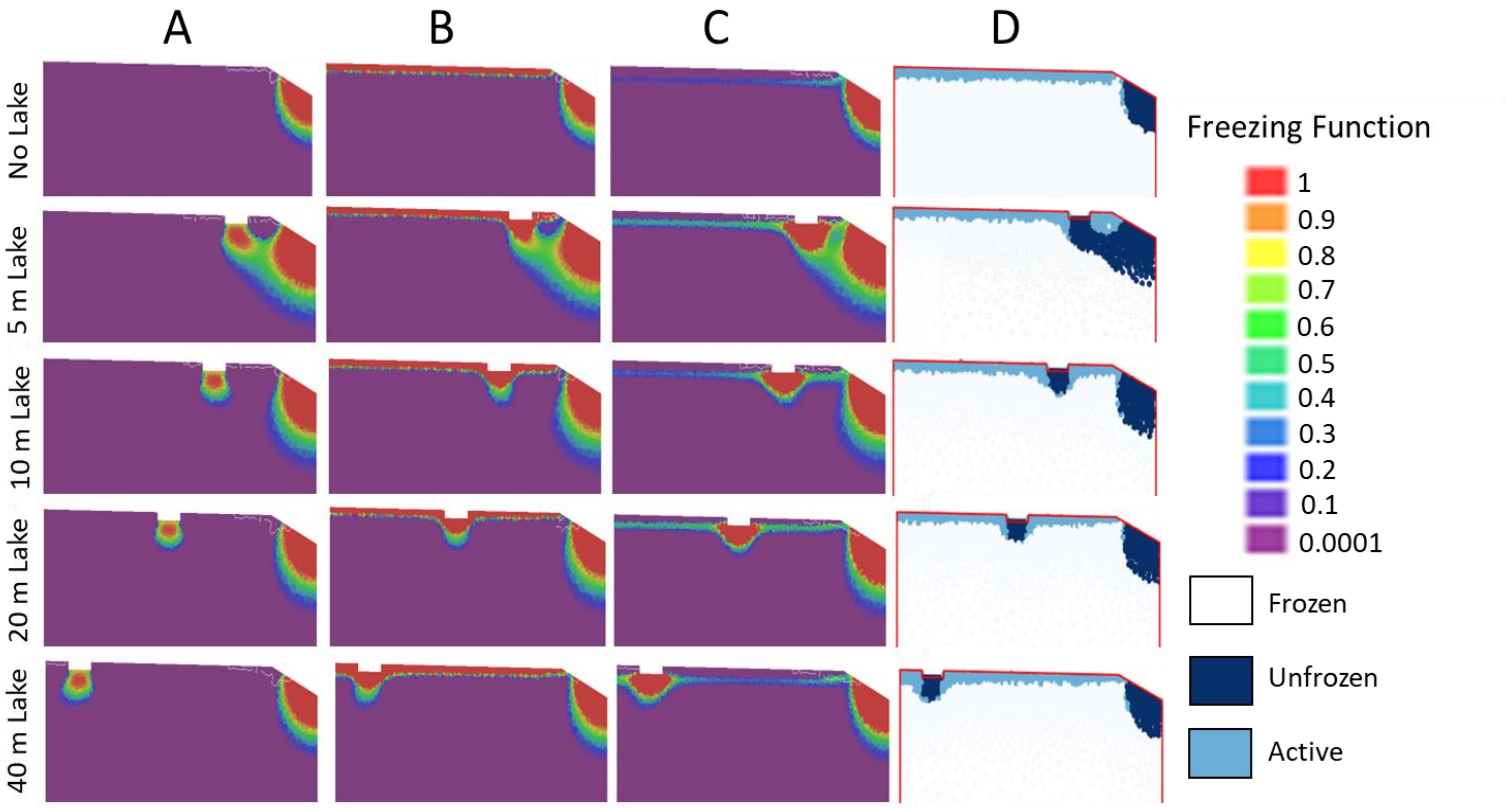

Figure 3. Seasonal change in aquifer freezing for No Lake, 5 m Lake, 10 m Lake, 20 m Lake, and 40 m lake from FEFLOW model simulations in columns A-C. Colors represent Freezing Function, where 1 (red) represents unfrozen (Temperature >1°C) and 0.0001 (purple) represents frozen (Temperature <-1°C) aquifer. Column D shows perennially frozen (white), perennially unfrozen (dark blue), and active (light blue) aquifer. Top half (upper 25 m) of each model simulation is shown.

Seasonal unfrozen aquifer area trends were similar across Lake model scenarios, but channel discharge varied with lake-channel distance (Figure 4). Both 20 m and 40 m Lake simulations had similar seasonal patterns in unfrozen area as perennial below-lake taliks contributed to consistent greater unfrozen area than in the No Lake model. Models with shorter

lake-channel distances (10 m and 5 m simulations) had larger unfrozen aquifer areas because of increased lake-channel connectivity through taliks increased the size of the channel talik (Figure 4A). The 5 m Lake had the greatest unfrozen aquifer area throughout the entire year due to the perennial lake-channel talik connection. Unfrozen aquifer area increases with increasing temperatures in the freshet and warm season as the unfrozen zone propagates downward (Figure 3C).

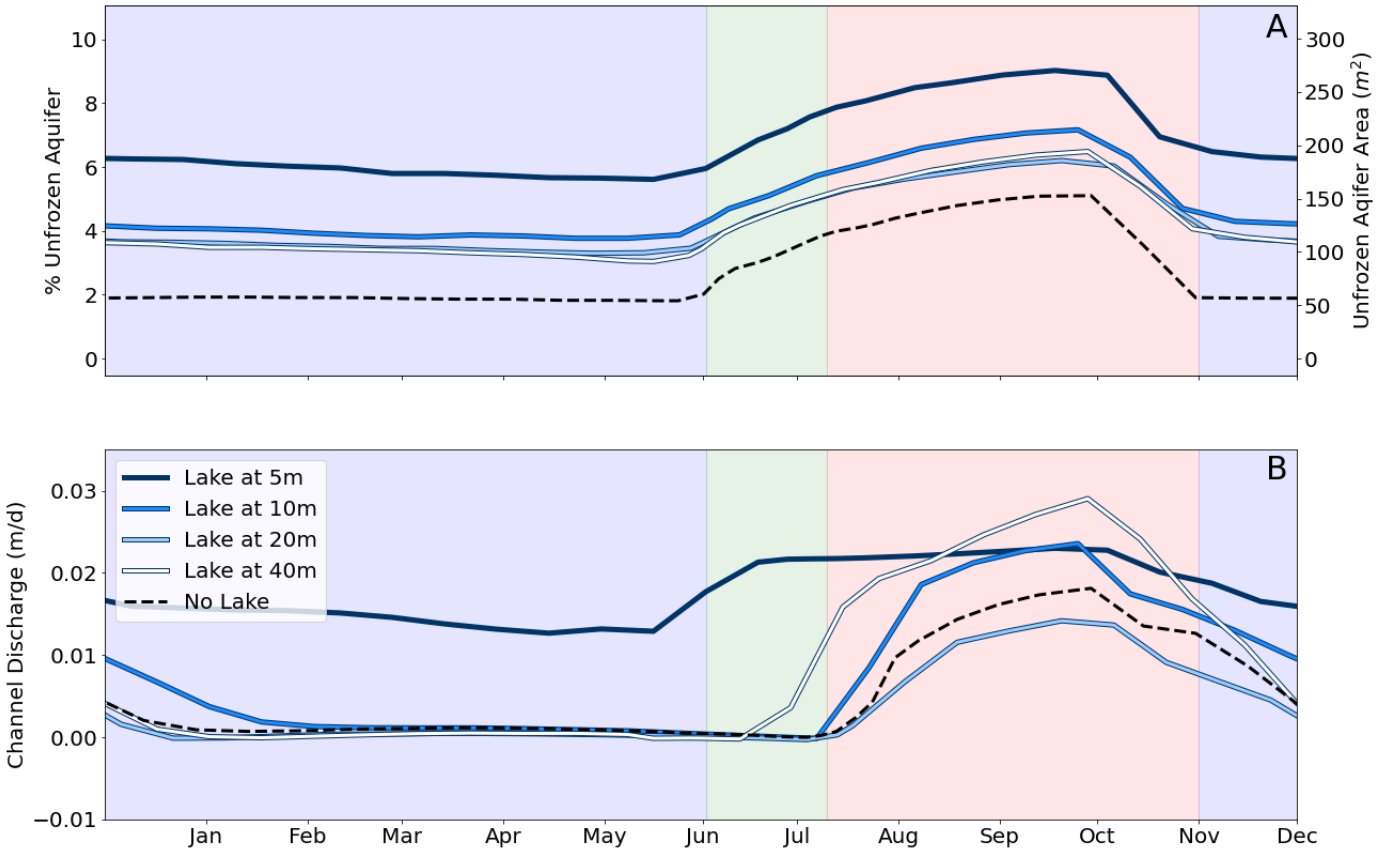

Figure 4. Annual time series of A) unfrozen aquifer percent and area change and B) flux to the channel from December 1-November 30.

As temperatures increase during the freshet, channel discharge begins to vary between model simulations. The 5 m Lake simulation has the greatest annual channel discharge of 0.45 m/yr while the 20 m Lake simulation has the least annual channel discharge of 0.08 m/yr. Lakes

serve as sources of recharge to the aquifer and as sinks to upgradient recharge. In the 40 m Lake simulation, with the smallest upgradient catchment area, most surface recharge discharges (along with lake recharge) directly to the channel contributing to high discharge rates. The 10 m Lake, with its large upgradient catchment, temporarily intercepts upgradient recharge before the active connection enables discharge to the channel. Additionally, as lake simulations increase distance from the channel, increased heat flux from the lake is isolated and contributes little to connectivity causing channel discharge to rely on increased temperatures during the warm season. While potential recharge enters the aquifer but the surficial aquifer and channel talik have yet to connect, much of the flux discharges through the drain above the channel, separate from channel discharge. As lake simulations decrease distance from the channel, connectivity occurs earlier and begins channel discharge in addition to the drain discharge above the channel. The 20 m lake simulation diverges from this pattern for multiple reasons. The 20 m Lake simulation had only 14% potential recharge enter the aquifer in addition to fairly equal upgradient and downgradient catchments which may have led to the decreased overall channel discharge. The 20 m Lake also allowed for delayed channel connection due to decreased heat flux due to greater distance which increased discharge to the drain rather than to the channel.

Channel discharge depends on unfrozen aquifer area and varies seasonally. Minimum unfrozen area immediately precedes freshet when sub-zero surface temperatures have persisted the longest (Figure 5). Increasing surface temperatures bring increased unfrozen area, but discharge to the channel stays low until the surface unfrozen zone connects to the channel talik, when it dramatically increases. Maximum discharge timing coincides with maximum unfrozen area. As surface temperatures decline and unfrozen area decreases back to mid-cold season minimum, channel discharge flux decreases until ultimately returning to minimal channel

recharge at times of minimum unfrozen area (Figure 4). These flow reversals which occur as the unfrozen zone refreezes correlates to flow reversals in talik closure in previous models (e.g. Scheidegger and Bense, 2014). All simulations but the 5 m lake show near-zero channel recharge at times of minimum unfrozen area. However, the 5 m lake simulation shows consistent discharge in addition to greatest unfrozen aquifer area.

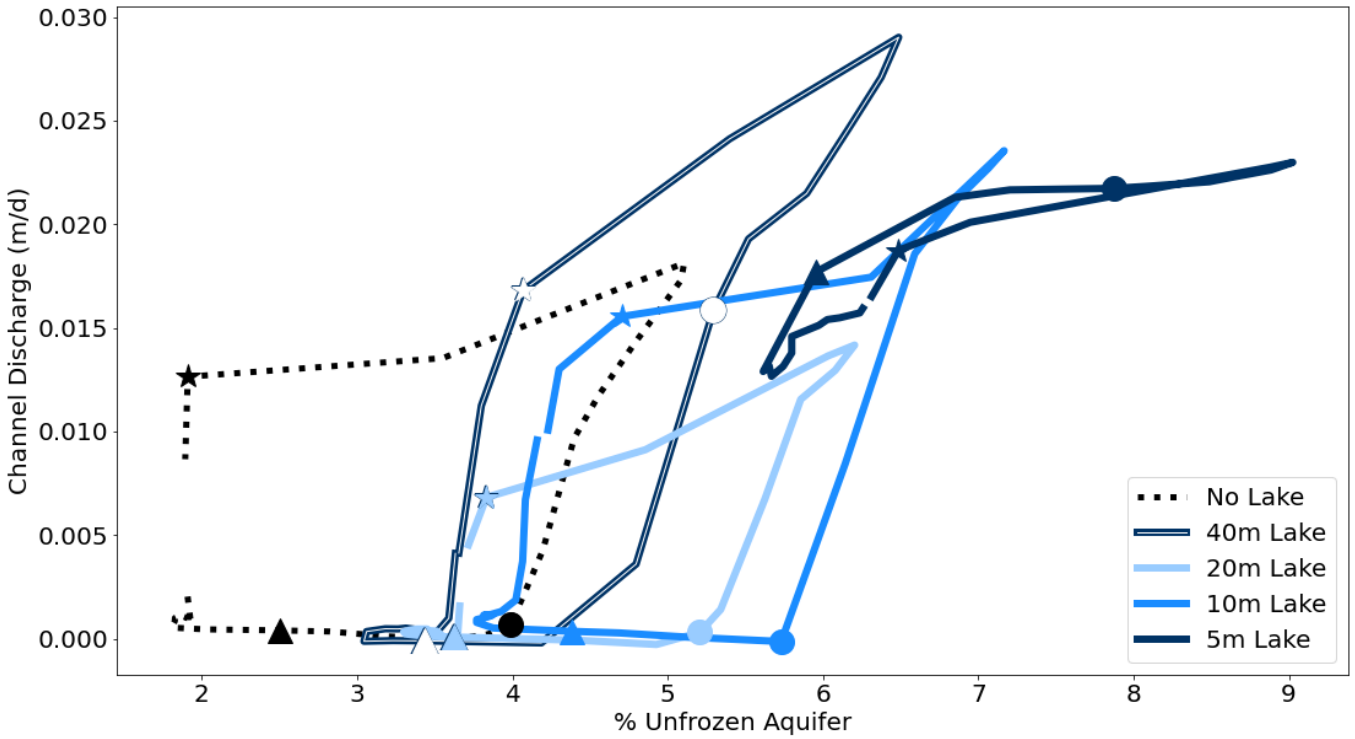

Figure 5. Annual unfrozen aquifer area and percentage comparison to channel discharge for 5 m, 10 m, 20 m, and 40 m, and No Lake simulations. Large markers of respective color of triangle, circle, and star represent start of the freshet, warm, and cold seasons respectively.

Model results suggest that channel-proximal lakes have increased heat transfer and connectivity which may be the primary mechanism driving near-channel lakes to shrink more quickly. As climate change continues to lengthen the warm season and shorten the cold season in

the Arctic, it is vital to understand how Arctic lakes may change with future climate scenarios. Surface water – groundwater models in permafrost settings deepens our understanding of spatial differential lake area shrinkage and increasing river baseflow in Arctic deltas and elucidates potential implications for Arctic ecosystems and the communities that depend on them.

It is important to acknowledge other factors that may influence channel discharge patterns as the Arctic continues to change under a warming climate. As temperatures increase, greater permafrost spatial variability will occur which may increase groundwater flow and decrease lake levels (Jepsen et al., 2013). However, increased permafrost meltwater may minimally affect groundwater discharge patterns as it is a relatively small contribution to surface water – groundwater connectivity (Walvoord and Kurylyk, 2020). Additionally, increased temperatures may decrease channel ice cover and reduce overbank flooding during the freshet (Lauzon et al., 2019). In this scenario, channel-proximal lakes may fail to obtain the large spring pulse of channel water and heat necessary for bank-full lakes and continued talik formation.

3.3.3 Sensitivity Analyses

Sensitivity analyses on No Lake models showed frozen area is most sensitive to temperature, channel discharge is most sensitive to K, and neither area nor discharge were sensitive to the potential recharge rate. Potential recharge rate had little effect on channel discharge or unfrozen aquifer area, because the aquifer quickly becomes fully saturated when restricted due to inhibiting permafrost and much of the potential recharge is lost to surface runoff (Figure 5A). The unfrozen aquifer area was most sensitive to the surface temperature signal amplitude – larger amplitudes increased the unfrozen area, and smaller amplitude decreased the unfrozen aquifer area (Figure 6B). Fluxes were relatively insensitive to temperature amplitude, but channel discharge was correlated with temperature amplitude, likely because of increased

aquifer transmissivity. Hydraulic conductivity had the greatest effect on channel discharge, decreasing the resistance to groundwater flow between the prescribed head lake and channel (Figure 6C). However, unfrozen area was insensitive to K.

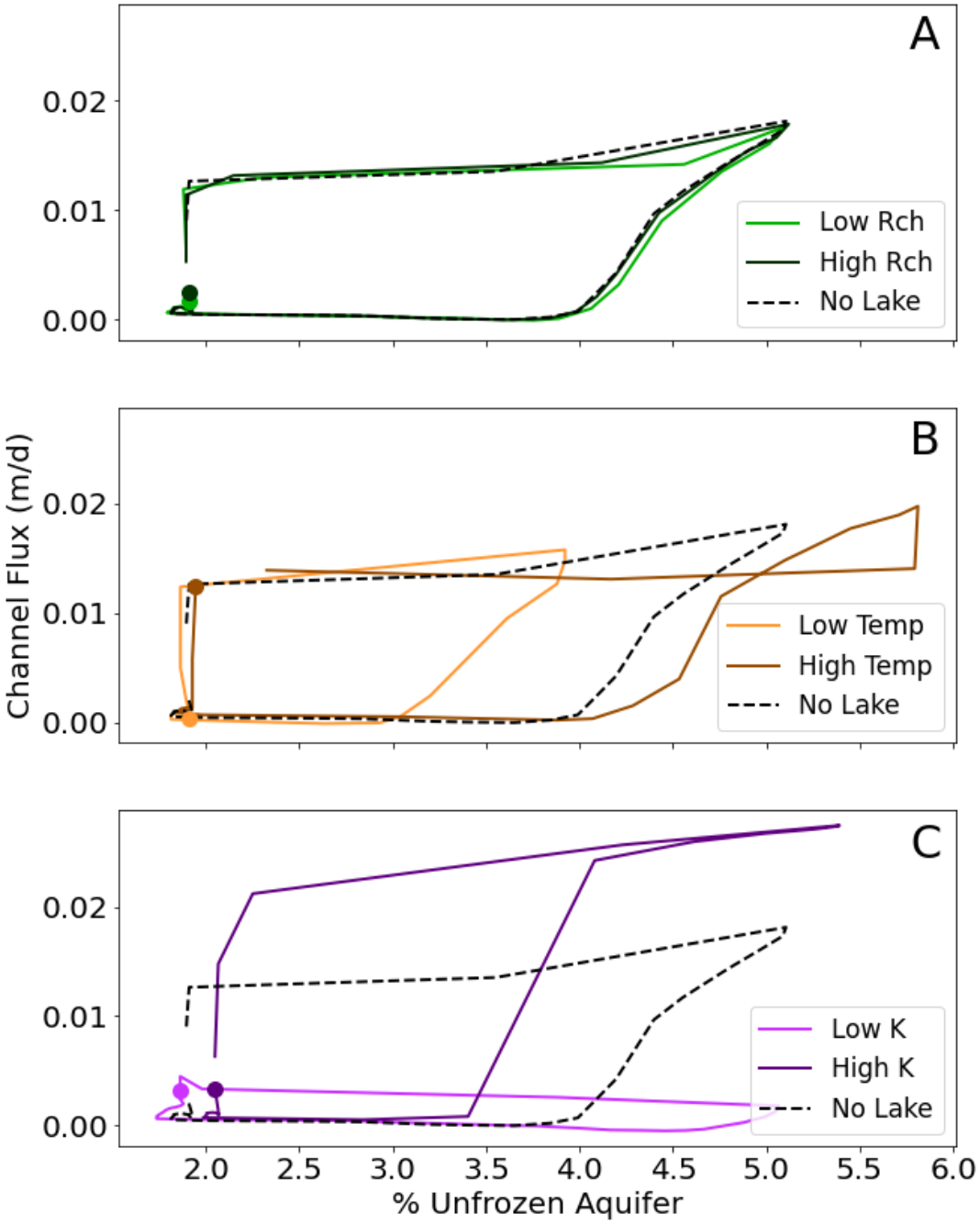

Figure 6. Model results from sensitivity analyses due to A) changing potential recharge, B) temperature amplitude, and C) hydraulic conductivity in one annual cycle compared to No Lake model. The dots of respective colors represent the starting point of the annual cycle on December 1. Note the shared x-axis for all plots.

3.4 Conclusions

The presence of a well-developed talik in near-channel lakes allows persistent lake-channel flow throughout the cold season– a mechanism that may explain why near-channel lakes shrink faster than lakes farther from channels. Lakes farther from the channel develop isolated, sub-lake taliks, however the consistent unfrozen pathway is critical for the drainage of these lakes to the channel. Shrinkage of lakes in deltas greatly depend on the groundwater pathways to downgradient channels which can be highly variable to seasonal temperatures and hydraulic conductivity.

Our study bridges the gap between these observations as near-channel lakes have greater channel discharge complimenting observed shrinkage. As near-channel lakes continue to have perennial channel discharge, lake flood water and solute residence time potential decrease. Decreased residence time has implications for solute processing potential and flood water storage. Increased channel discharge may lead to coastal flooding as well as harmful algal blooms due to unprocessed solutes, which can be detrimental to the fragile Arctic ecosystems. To better understand these systems further, future work may include the addition of reactive solute transport as well as simulations under climate change warming scenarios.

Chapter 4: Challenges and Future Work

As many modeling projects go, this project was not without its challenges. Modeling unsaturated flow and heat transfer with an additional complexity of freeze thaw makes each model calculation highly intensive. Due to these complex calculations, model simulations had to be a balance between spatial discretization and acceptable run time length. Initial model discretization used FEFLOW's Triangle mesh with a target mesh size of 0.1 m at the surface with a gradual mesh size increase with domain depth. These initial models not only could take over two weeks to complete a few years of model simulation, but also would experience propagating numerical issues. For example, when the talik would begin to close at the start of the cold season, extremely low heads at a few problematic nodes would dramatically change the flow directions and simulate unrepresentative flow reversals. Our plan to mitigate this issue with finer spatial discretization only amplified the issue and either had extremely long run times, or simply crashed mid-way through a 5-year simulation. To see if this problem would converge on a solution with longer run times, spatial discretization was coarsened to a target mesh size of 1 m at the domain surface with a gradual mesh size increase with domain depth. Coarsening spatial discretization dramatically decreased model run times to ~4 days for a 50-year simulation and made the magnitude of flow reversals (near zero) much more manageable.

With the coarsening of spatial discretization, model error budgets increased outside of acceptable limits. In an attempt to lower model error budgets, both Equation-System Solver and temporal discretization were adjusted. Adjusting the Equation-System Solver from the default Standard Iterative method (PCG) to the Direct or Algebraic Multigrid (SAMG) solvers had little to no observed change. Temporal discretization could be changed from Automatic time-step control to Constant time steps or Varying time steps. However, as high stress periods such as the

freshet cause times of complex calculations, time steps automatically decrease to lower model error, and during constant periods such as the cold season when there is no recharge, time steps automatically increase to a user-defined maximum to decrease model run time when using Automatic time-step control. Constant time steps or Varying time steps are user-defined, and do not have the capability to adjust to stress periods unless proactively determined. Thus, Automatic time-step control is the ideal choice for model simulations.

FEFLOW has extensive online documentation and tutorials, however, remains convoluted and "black-box" to the novice user. FEFLOW is constantly updating, where some capabilities are only available in certain versions but remain in the documentation. Additionally, FEFLOW is entirely GUI-based, so determining issues within the model remain difficult to pin-point. Because of this, extracting data continued to be difficult as each parameter would need to be manually saved, where for example magnitude and direction of flow would not be saved in the same parameter, and some parameters could only be accessed through FEFLOW's Python package. FEFLOW's Python package (ifm) allows model simulations to run and extract outputs through any Python interface. However, the ifm package does not yet support the capabilities of piFreeze, which is a crucial component of this modeling project. When questions arise with software difficulties, FEFLOW does host online forums to obtain help from the developers. However, many forum threads with questions are asked publicly, but answered privately with no posted answer for users with similar questions. FEFLOW is also a highly expensive software package and only remains affordable for users with a free student license. The cost of FEFLOW greatly inhibits other researchers from using the program, thus decreasing scientific communication and trouble-shooting opportunities. For researchers who wish to expand upon

this work, the use of SUTRA-ICE or another open-source program with freeze-thaw capabilities is recommended.

There are many options for future work stemming from these preliminary models. To begin, if models are created in SUTRA-ICE, then models can use exact boundary conditions as Lamontagne-Halle et. al., (2016) as this model could not consider same drain and snow insulation boundary conditions at the surface. Once this model has more realistic boundary conditions, then a thorough comparison of results between Lake models and the Lamontagne-Halle et al., (2016) models can be conducted. Lamontagne-Halle et. al., (2016) also included the rise of mean temperature through time to simulate climate warming. The addition of climate warming with future work is crucial for understanding how delta lake-channel connectivity will affect groundwater discharge. As the warm season becomes longer and hotter, the shorter cold season will not be able to completely refreeze the warm season connectivity, thus perennial taliks may develop at further lake distances such as 10 or 20 m.

As climate change also continues to change ice-melt dynamics and delta morphology, the magnitude of the spring freshet may be confined to the channels rather than flooding channel banks into nearby lakes (Lauzon et al., 2019). To understand how groundwater discharge to downgradient channels may be affected by the absence of spring flooding events at the surface, future models may simulate lake and channel hydraulic head boundary conditions as time-varying rather than constant. A time-varying hydraulic head boundary condition may display the possibility of flow reversals from the channel to thermokarst lakes during times of high head in the channel and low head in the shrinking lakes which has been observed in other karst regions (e.g. Hensley and Cohen, 2017).

Perennial flux from near-channel lakes has the potential to decrease lake residence times, thus decreasing nutrient processing potential (Emmerton et. al., 2008). To understand the importance of these lakes with regard to nutrient processing, additional simulations may be conducted with reactive transport. Quantifying reactive transport with lake-channel proximity may show less-connected lakes with higher residence times have greater processing potential, which allow for less harmful nutrient flux to enter the arctic seas.

Lastly, future models may include the addition of coastal flooding and saltwater-induced permafrost melt. As climate change continues, the frequency of severe storms will likely increase, so it is important to consider the effects of rising seas, storm surge, and saltwater intrusion on talik formation within arctic deltas. Intrusion of warm saline waters into frozen aquifers promotes initial thawing, and recent work shows the depressed freezing point drives positive feedback (Guimond et al., 2021). Both remote sensing and modeling analyses would clarify these processes, such as mapping coastal flooding extent due to storm surge within arctic deltas and modeling salt-water induced permafrost melt. Thermokarst lakes affected by storm surge can be identified by calculating volume change pre- and post- storm event by using NASA's open-source Surface Water and Ocean Topography (SWOT) satellite mission. After the volume of saltwater inundation has been calculated, models can use this pulse event as initial conditions to simulate saltwater influence on talik formation. Understanding saltwater influence on permafrost thaw in arctic deltas was recently proposed to the NSF GRFP and received positive reviews.

References

Aagaard, K., & Carmack, E. C. (1989). The role of sea ice and other fresh water in the Arctic circulation. *Journal of Geophysical Research: Oceans*, *94*(C10), 14485-14498.

ACIA, 2004. Impacts of a Warming Arctic: Arctic Climate Impact Assessment. ACIA Overview report. Cambridge University Press. 140 pp.

Arp, C. D., B. M. Jones, G. Grosse, A. C. Bondurant, V. E. Romanovsky, K. M. Hinkel, and A. D. Parsekian (2016), Threshold sensitivity of shallow Arctic lakes and sublake permafrost to changing winter climate, Geophys. Res. Lett., 43, 6358–6365, doi:10.1002/2016GL068506.

Burn, C. R., (2003) Lake-bottom thermal regime in thermokarst terrain near Mayo, Yukon Territory, Canada *Proc. 8th Presented Int. Conf. Permafrost, 21–25 July, 2003* (Zurich) pp 113–18

Burn, C.R. (2005) Lake-bottom thermal regimes, western Arctic coast, Canada. Permafrost Periglacial Process. 16:355–367. doi:10.1002/ppp.542

Dimova, N.T., Paytan, A., Kessler, J. D., Sparrow, K. J., Kodovska, F, G-T., Lecher, A. L., Murray, J., and S. M. Tulaczyk (2015), Current Magnitude and Mechanisms for Groundwater Discharge in the Arctic: Case Study from Alaska, Environmental Science and Technology, 49, 12036-12043, doi: 10.1021/acs.est.5b02215.

Emmerton, C. A., Lesack, L. F. W., and Marsh, P. (2007), Lake abundance, potential water storage, and habitat distribution in the Mackenzie River Delta, western Canadian Arctic, *Water Resour. Res.*, 43, W05419, doi:10.1029/2006WR005139.

Emmerton, C. A., L. F. W. Lesack, and W. F. Vincent (2008), Mackenzie River nutrient delivery to the Arctic Ocean and effects of the Mackenzie Delta during open water conditions, Global Biogeochem. Cycles, 22, GB1024, doi:10.1029/2006GB002856.

Guimond, J.A., Mohammed, A. A., Walvoord, M. A., Bense, V. F., & Kurylyk, B. L, (2021). Saltwater intrusion intensifies coastal permafrost thaw. Geophysical Research Letters, 48, e2021GL094776.

Hensley, R.T., and Cohen, M. J. (2017), Flow reversals as a driver of ecosystem transition in Florida's springs, *Freshwater Science*, 36(1):000—000, doi:10.1086/690558.

Holland, M. M., Finnis, J., Barrett, A. P., & Serreze, M. C. (2007). Projected changes in Arctic Ocean freshwater budgets. *Journal of Geophysical Research: Biogeosciences*, *112*(G4).

Holmes, R. M., Peterson, B. J., Zhulidov, A. V., Gordeev, V. V., Makkaveev, P. N., Stunzhas, P.

A., & Shiklomanov, A. I. (2001). Nutrient chemistry of the Ob'and Yenisey Rivers, Siberia: Results from June 2000 expedition and evaluation of long-term data sets. *Marine Chemistry*, *75*(3), 219-227.

Holmes, R.M., McClelland, J.W., Peterson, B.J. (2012), Seasonal and Annual Fluxes of Nutrients and Organic Matter from Large Rivers to the Arctic Ocean and Surrounding Seas. *Estuaries and Coasts* 35, 369–382. https://doiorg.wvu.idm.oclc.org/10.1007/s12237-011-9386-6.

Jepsen, S. M., Voss, C. I., Walvoord, M. A., Minsley, B. J., and Rover, J. (2013), Linkages between lake shrinkage/expansion and sublacustrine permafrost distribution determined from remote sensing of interior Alaska, USA, *Geophys. Res. Lett.*, 40, 882– 887, doi:10.1002/grl.50187.

Jorgenson, M. T., Y. L. Shur, and E. R. Pullman (2006), Abrupt increase in permafrost degradation in Arctic Alaska, Geophys. Res. Lett., 33, L02503, doi:10.1029/2005GL024960.

Kurylyk BL, Irvine DJ, Bense VF. Theory, tools, and multidisciplinary applications for tracing groundwater fluxes from temperature profiles. WIREs Water. 2019;6:e1329. https://doi.org/10.1002/wat2.1329KURYLYK ET AL.

Lamontagne-Hallé, P., McKenzie, J. M., Kurylyk, B. L., & Zipper, S. C. (2018). Changing groundwater discharge dynamics in permafrost regions. Environmental Research Letters, 13(8). https://doi.org/10.1088/1748-9326/aad404

Lauzon, R., Piliouras, A., & Rowland, J. C. (2019). Ice and permafrost effects on delta morphology and channel dynamics. *Geophysical Research Letters*, *46*(12), 6574–6582. https://doi.org/10.1029/2019gl082792

Marsh, P., and M. Hey (1989), The flooding hydrology of Mackenzie Delta lakes near Inuvik, NWT, Canada, Arctic, 42(1), 41 –49.

Mckenzie, Jeff & Voss, Clifford. (2013). Permafrost thaw in a nested groundwater-flow system. Hydrogeology Journal. 21. 10.1007/s10040-012-0942-3.

MIKE (2016). piFreeze, A Freeze/Thaw Plug-in for FEFLOW User Guide.

National Centers for Environmental Information (NCEI). "Daily Summaries Station Details." *Daily Summaries Station Details: BARROW AIRPORT, AK US, GHCND: USW00027502 | Climate Data Online (CDO) | National Climatic Data Center (NCDC),* https://www.ncdc.noaa.gov/cdo-web/datasets/GHCND/stations/GHCND:USW00027502/detail.

Nitze, I., Grosse, G., Jones, B.M., Arp, C.D., Ulrich, M., Fedorov, A., Veremeeva, A. (2017),

Landsat-Based Trend Analysis of Lake Dynamics across Northern Permafrost Regions. *Remote Sensing*. 2017; 9(7):640. https://doi.org/10.3390/rs9070640.

Piliouras, A., & Rowland, J. C. (2020). Arctic river delta morphologic variability and implications for riverine fluxes to the coast. Journal of Geophysical Research: Earth Surface, 125, e2019JF005250. https://doi.org/10.1029/2019JF005250

Piliouras, A., Lauzon, R., & Rowland, J. C. (2021). Unraveling the combined effects of ice and permafrost on Arctic delta morphodynamics. *Journal of Geophysical Research: Earth Surface*, *126*, e2020JF005706. https://doi.org/10.1029/2020JF005706

Rau, G.C., Andersen, M.S., McCallum, A.M., Roshan, H.,Acworth, R.I. (2014), Heat as a tracer to quantify flow in near-stream sediments. Earth-Science Reviews 1 29: 40-58, doi:10.1016/j.earscirev.2013.10.015.

Rowland, Joel & Travis, Bryan & Wilson, Cathy. (2011). The Role of Advective Heat Transport in Talik Development Beneath Lakes and Ponds in Discontinuous Permafrost. AGU Fall Meeting Abstracts. 38. 01-. 10.1029/2011GL048497.

Scheidegger, J. M., and V. F. Bense (2014), Impacts of glacially recharged groundwater flow systems on talik evolution, J. Geophys. Res. Earth Surf., 119,758–778, doi:10.1002/2013JF002894.

St. Jacques, J.-M., and Sauchyn, D. J. (2009), Increasing winter baseflow and mean annual streamflow from possible permafrost thawing in the Northwest Territories, Canada, *Geophys. Res. Lett.*, 36, L01401, doi:10.1029/2008GL035822.

Vulis, L., Tejedor, A., Schwenk, J., Piliouras, A., Rowland, J., & Foufoula-Georgiou, E. (2020). Channel network control on seasonal lake area dynamics in arctic deltas. *Geophysical Research Letters*, 47, e2019GL086710. https://doi.org/10.1029/2019GL086710.

Whalen, D., Forbes, D.L., Hopkinson, C., Lavergne, J.C., Manson, G.K., Marsh, P., Solomon, S.M. (2009), Topographic LiDAR - providing a new perspective in the Mackenzie Delta, Proceedings of the 30th Canadian Symposium on Remote Sensing.

Walvoord, M.A. and Kurylyk, B.L. (2016), Hydrologic Impacts of Thawing Permafrost—A Review. Vadose Zone Journal, 15: 1-20 vzj2016.01.0010. https://doi.org/10.2136/vzj2016.01.0010

Yang, D., Marsh, P., Ge, S. (2014), Heat flux calculations for Mackenzie and Yukon Rivers. Polar Science. 8, 232-241, http://dx.doi.org/10.1016/j.polar.2014.05.001

You Y, Yu Q, Pan X, Wang X, Guo L,Wu Q. Thermal effects of lateral supra-permafrost water flow around a thermokarst lake on the Qinghai–Tibet Plateau. Hydrological Processes. 2017; 31:2429–2437. https://doi.org/10.1002/hyp.11193

Supplemental

Figures

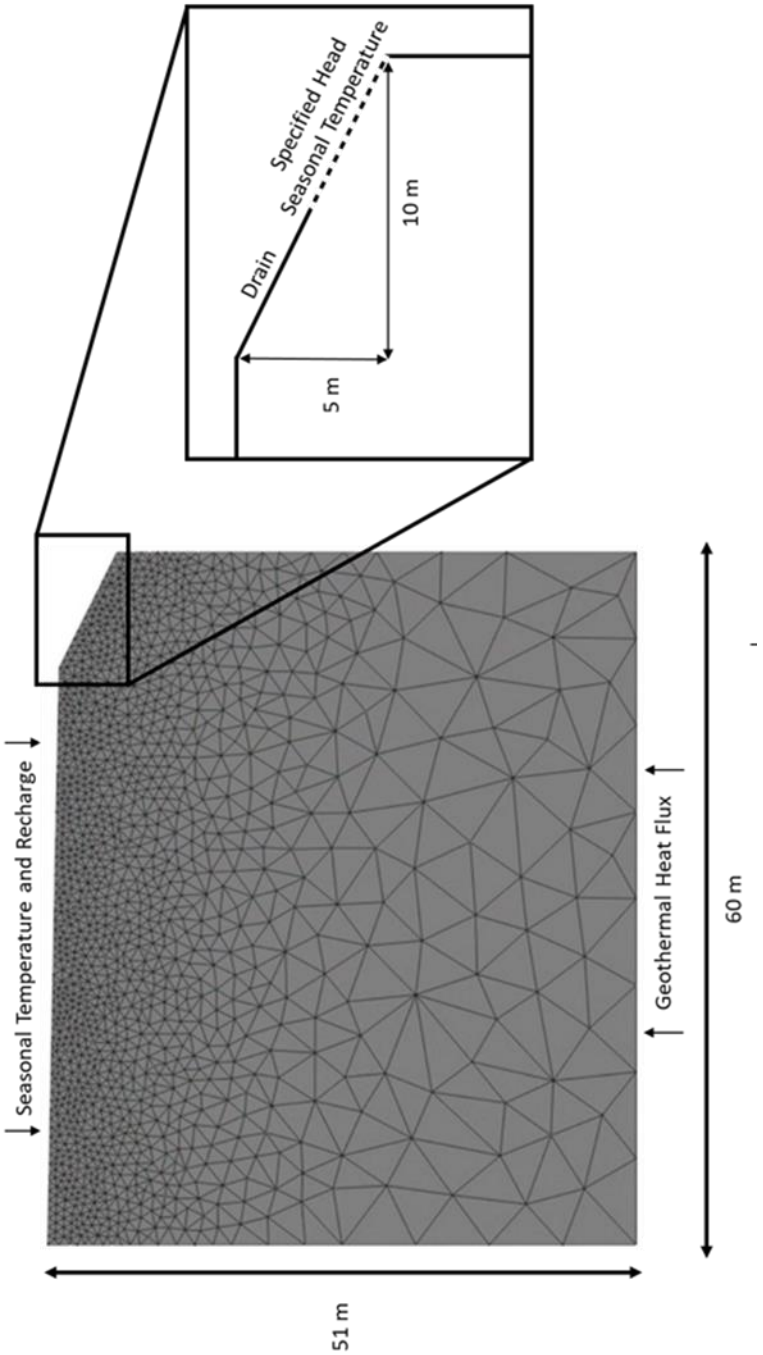

Figure S1. No Lake domain geometry with associated discretization and boundary conditions.

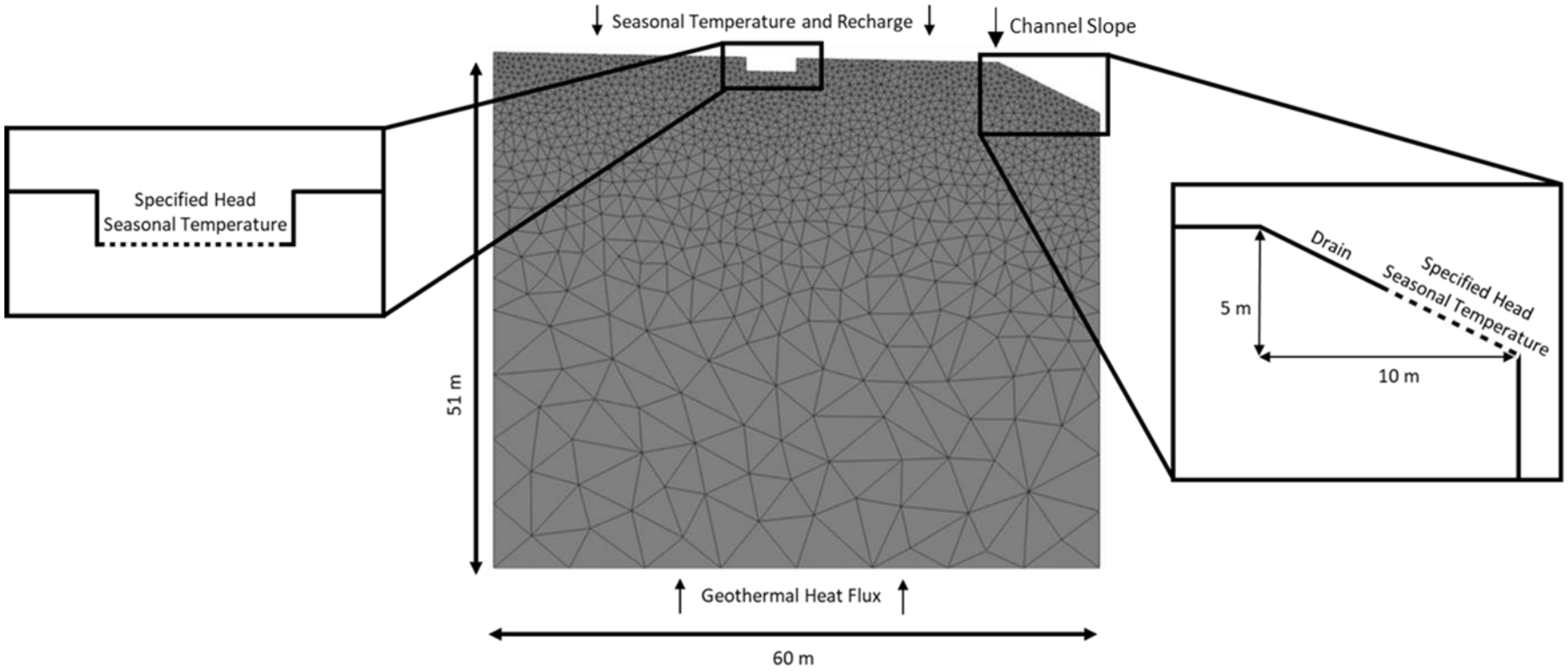

Figure S2. Lake model domain geometry with associated discretization and boundary conditions. Lake models contain same boundary conditions; however, location of the lake's right bank varies from 5, 10, 20, and 40 m from the channel slope. The 20 m lake is shown above.

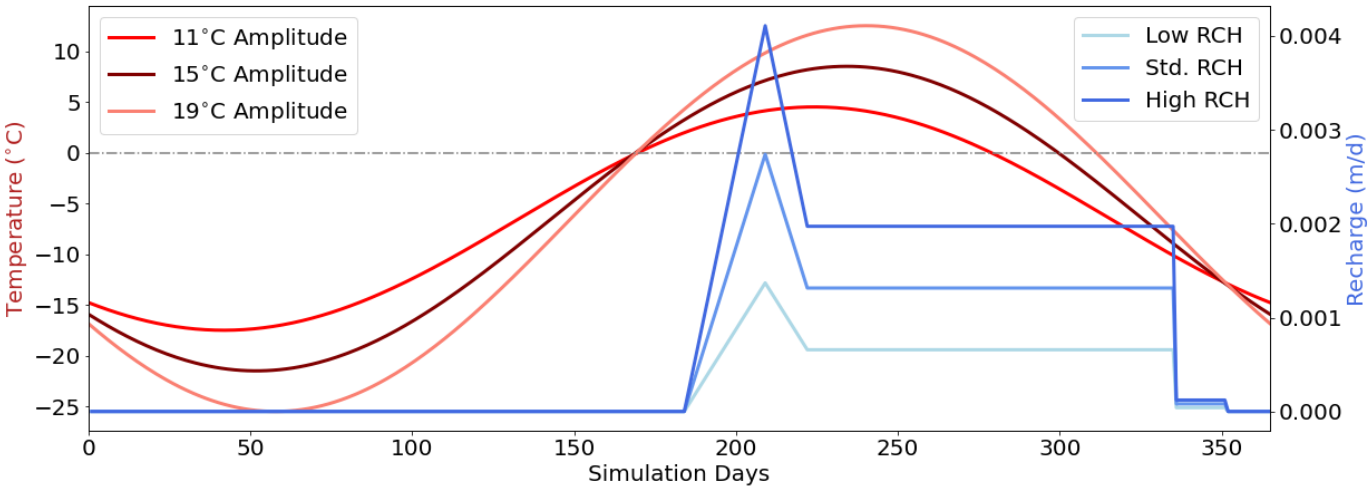

Figure S3. Temperature and recharge time series during sensitivity analyses. Temperature amplitudes were adjusted to 11°C (Low temperature), 15°C (Standard temperature), or 19°C (High temperature); however, each temperature time series increases above 0°C 15 days before the spring freshet. Average annual recharge was adjusted to 0.1 m/yr (Low RCH), 0.2 m/yr (Std. RCH) or 0.3 m/yr (High RCH).

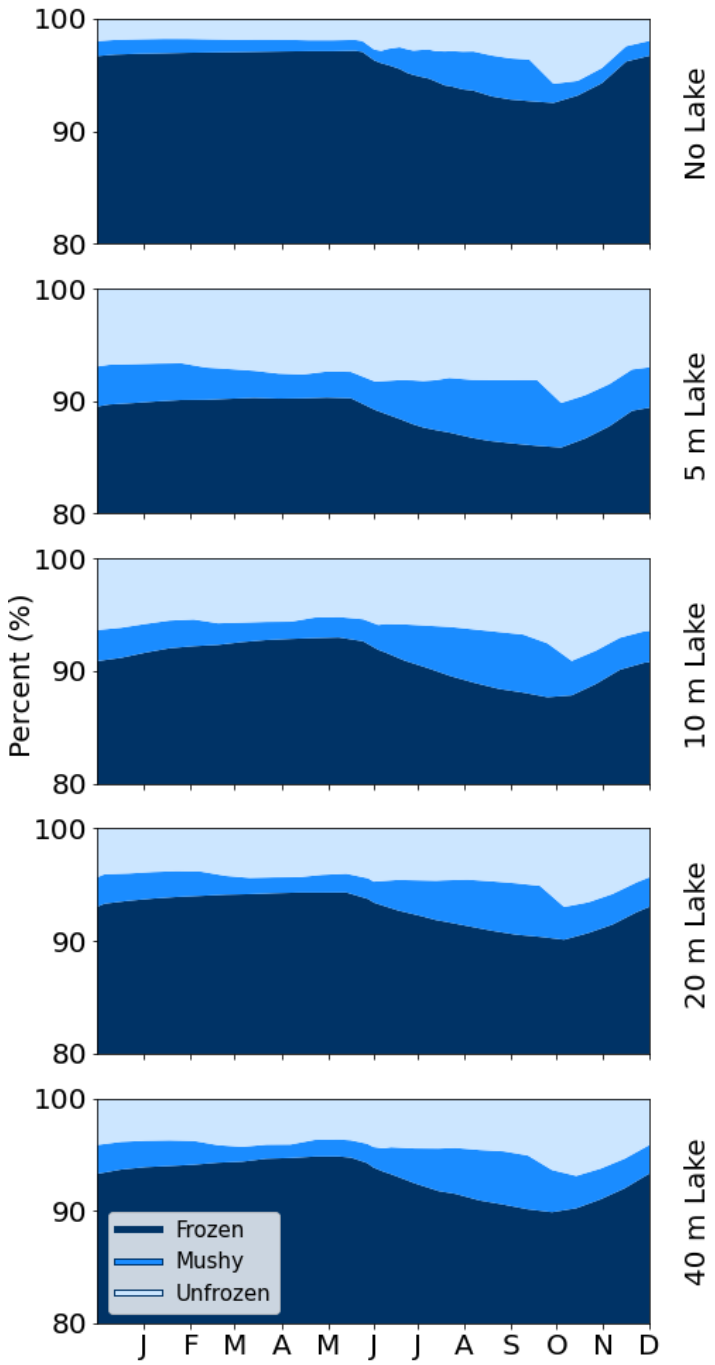

Figure S4. Stacked plot of changing percentage of frozen (Temperature <-1°C), slushy (-1°C < Temperature <1°C), or unfrozen (Temperature >1°C) aquifer for 1 year. Note the shared x-axis.

Figure S5. Field location view of temperature profile. View South from Cakeeatter Road.

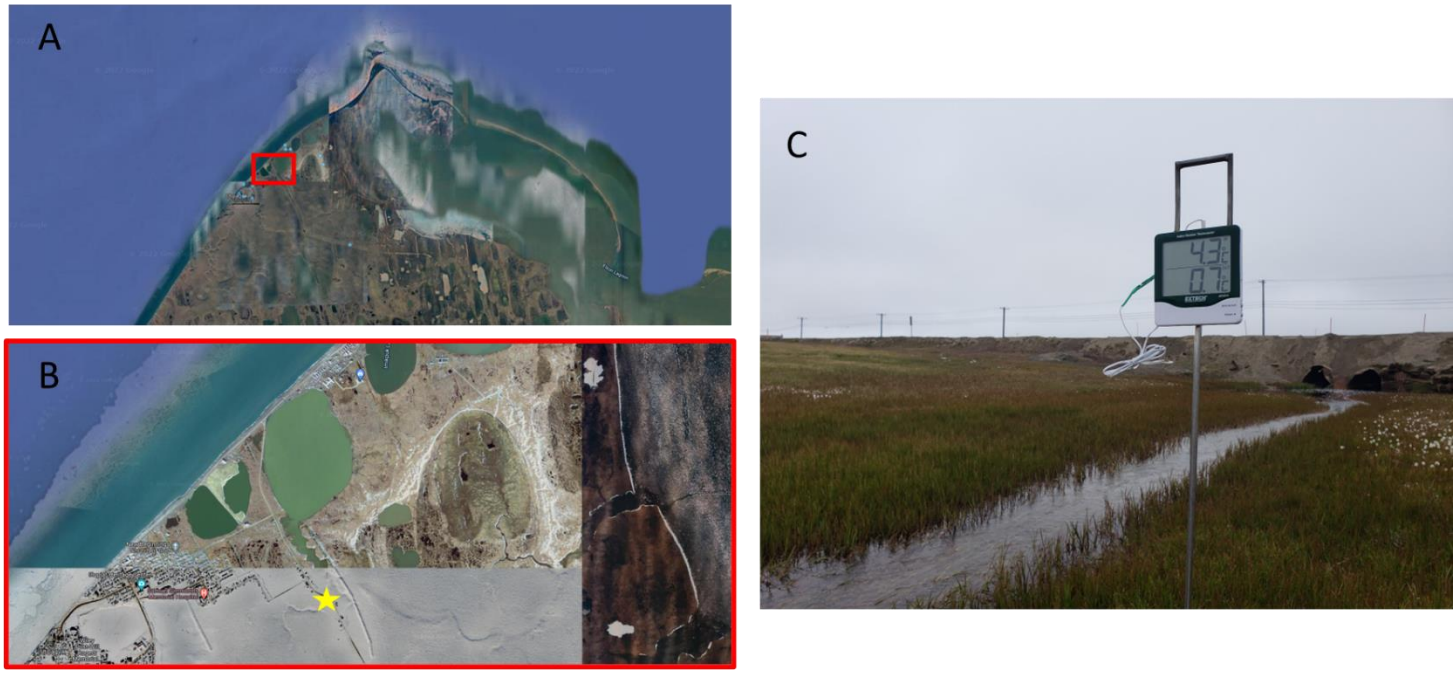

Figure S6. Cross-sectional temperature profile map southeast of Utqiagvik, AK. Panel A shows northern Alaska, with the northern-most point as Point Barrow, AK. Red box in Panel A shows relative location of Panel B. Starred location in Panel B shows location of cross-sectional temperature profile along Cakeatter Road (71° 17’51.6”, 156° 40’ 51.9”). Panel C shows the location from the profile view North towards Cakeatter Road.

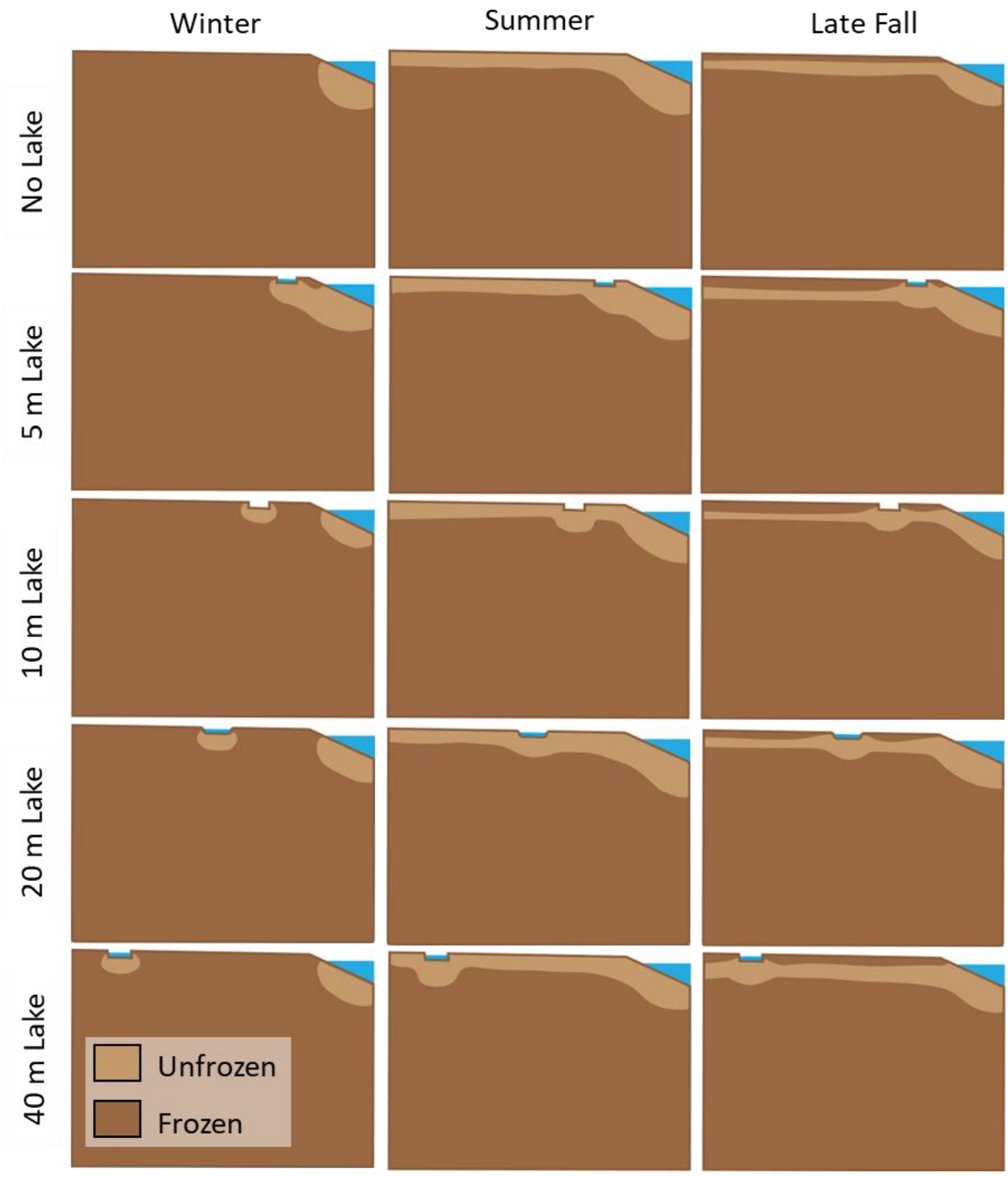

Figure S7. Conceptual model to display lake-channel connectivity through the winter, summer, and late fall.

Tables

Table S1. Model Parameters.

Model Parameters		
Parameter	Unit	Value
Hydraulic Conductivity	[m/d]	0.09
Porosity	[ ]	0.1
Specific Storage	[1/m]	0.0001
Fluid Thermal Conductivity	[J/m/s/k]	0.6
Solid Thermal Conductivity	[J/m/s/k]	3.5
Ice Thermal Conductivity	[J/mdk]	184896
Fluid Volumetric Heat Capacity	[MJ/m^3/K]	4.2
Solid Volumetric Heat Capacity	[MJ/m^3/K]	1.94
Ice Volumetric Heat Capacity	[J/m^3/K]	2184000
Latent Heat of Fusion	[J/kg]	334000
Liquid Density	[kg/m^3]	1000
Ice Density	[kg/m^3]	917.5
Residual Liquid Fraction	[ ]	0.0001
Longitudinal Dispersivity	[m]	5
Transverse Dispersivity	[m]	0.5

Table S2. Model parameter values adjusted during sensitivity analyses.

Parameter	Low	Standard	High
Recharge (m/yr)	0.1	0.2	0.3
Hydraulic Conductivity (m/d)	0.009	0.09	0.9
Temperature Amplitude (°C)	11	15	19

Table S3. Model Simulations.

Models								
Model Name	Hydraulic Condictivity [m/d]	Recharge [m/yr]	Temp Amplitude [C]	Residual Liquid Fraction	Observation Point X	Observation Point Y	Final Simulation Time	Notes
Base009	0.09	NaN	NaN	0.0001			1.095E+07	SS Temp before Time Series
Base009_2	0.09	NaN	NaN	0.025			1.095E+07	SS Temp before Time Series
Base09	0.9	NaN	NaN	0.0001			1.095E+07	SS Temp before Time Series
Base0009	0.009	NaN	NaN	0.0001			1.095E+07	SS Temp before Time Series + NearLake
42222m2	0.09	NaN	NaN	0.0001				Base for far lake
42122M1	0.09	NaN	NaN	0.0001			1.095E+07	SS Temp before Time Series
4722M1	0.09	0.2	20	0.0001			17217	Base Model High Temp
4722M2	0.09	0.2	15	0.025			16150	Base Model Base Temp low RLF
4922M1	0.09	0.2	20	0.0001	49.822	48.003	19801	Base Model High Temp + Observation pt
4922M2	0.09	0.2	15	0.025	49.822	48.003	21006	Base Model Base Temp low RLF +Observation pt
41222BarM1	0.09	0.2	15	0.0001	49.822	48.003	7134.93	Barrow Temperature Series, No Lake // died mid simmy
41322M1	0.9	0.2	15	0.0001	49.822	48.003	1673	died mid simmy
41422BarM1_1	0.09	0.2	15	0.0001	49.822	48.003		Barrow Temperature Series, No Lake
41422M1	0.9	0.2	15	0.0001	49.822	48.003	29676	Base Model high K
41922m1	0.09	0.2	11	0.0001	50	48	18642	Base Model low temp
41922m2	0.09	0.2	15	0.0001	50	48	20808	Base Model (other pc)
41922M4	0.009	0.2	15	0.0001	50	49	19752	Base Model, low K
42022m1	0.09	0.1	15	0.0001	50	48	36500	Base Model, low recharge

42022m2	0.09	0.3	15	0.0001	50	48	36500	Base model, high recharge
42022m3	0.09	0.2	15	0.0001	50	48		Base Model
42122M2	0.09	0.2	15	0.0001	50	48		Near Lake Model 1
42222m1	0.09	0.2	19	0.0001	50	48		Base Model, High temp
42322m1	0.09	0.2	15	0.0001	50	48		Far Lake Model 1
42922m1	0.09	0.1	15	0.0001	50	48	never started	changing recharge from fluid flux to inflow ; copy of 42022m1
5422m1	0.09 (0.0009 below lake)	nAn	nan	0.0001				base model with low k beneath lake
5422m2	0.09 (0.0009 below lake)	0.2	15	0.0001	50	48		base model with low k beneath lake transient simmy
5522m1								Lamontage-halle conditions
5922m1	0.09	nan	nan	0.0001	50	48		new base model with fixed K vals beneath channel
5922m2	0.09	0.2	19	0.0001	x	x	18250	new high temp model with fixed high temp and K vals beneath channel
5922m3	0.09	0.2	15	0.0001			18250	new base model with fixed temp and K vals beneath channel
5922m4	0.09	0.2	11	0.0001			18250	new low temp model with fixed temp and K vals beneath channel
5922m5	0.09	0.1	15	0.0001			18250	new low rch model with fixed temp and K vals beneath channel
51122m1	0.09 (0.0009 beneath channel and lake)	0.2	15	0.0001			18250	new near lake model with fixed temps
51122m2	0.09 (0.0009	0.2	15	0.0001			18250	new far lake model with fixed temps

	beneath channel and lake)							
51122m3	0.09 (0.0009 beneath channel and lake)	0.2	15	0.0001			18250	new high recharge model with fixed temps
51422m1	0.09 (0.0009 beneath channel and lake)	0.2	15	0.0001			18250	closest lake model
51422m2	0.09 (0.0009 beneath channel and lake)	0.2	15	0.0001			18250	near lake model with no heat beneath lakes for ss permafrost ?? Accicdentally ran to wrong end time
51622m1	0.09 (0.0009 beneath channel and lake)	0.2	15	0.0001			18250	far lake model with no heat beneath lakes for ss permafrost
51622m2	0.09 (0.0009 beneath channel and lake)	0.2	15	0.0001			18250	closest lake model with no heat beneath lakes for ss permafrost
51622m3	0.09 (0.0009 beneath channel and lake)	0.2	15	0.0001			18250	near lake model with no heat beneath lakes for ss permafrost ; lake head to top of domain (yloc = 1.37)
51622m4	0.09 (0.0009 beneath channel and lake)	0.2	15	0.0001			18250	closest lake model with no heat beneath lakes for ss permafrost ; lake head to top of domain (yloc = 1.37)
51722m1	0.09 (0.0009 beneath channel	0.2	15	0.0001			18250	base model with no temp during ss and fixed temp

	and lake)							
51922m1	0.09 (0.0009 beneath channel and lake)	0.2	15	0.0001			18250	far lake model with no heat beneath lakes for ss permafrost ; lake head to top of domain (yloc = 1.37)
51922m2	0.09 (0.0009 beneath channel and lake)	0.2	15	0.0001			18250	low rch base model with no temp during ss and fixed temp
51922m3	0.09 (0.0009 beneath channel and lake)	0.2	15	0.0001			18250	high rch base model with no temp during ss and fixed temp
52122m1	0.09 (0.0009 beneath channel and lake)	0.2	15	0.0001			18250	10 m lake from channel slope head at lake base
52122m2	0.09 (0.0009 beneath channel and lake)	0.2	15	0.0001			18250	10 m lake from channel slope head +1.37 from base
52222m1	0.09 (0.0009 beneath channel and lake)	0.2	15	0.0001			18250	low temp
52222m2	0.09 (0.0009 beneath channel and lake)	0.2	15	0.0001			18250	high temp
53022m2	0.009 (0.0009 beneath channel and lake)	0.2	15	0.0001			18250	low k

53022m1	0.9 (0.0009 beneath channel and lake)	0.2	15	0.0001			18250	high k

Python Code

FEFLOW Boundary Conditions: https://colab.research.google.com/drive/1LD0-UJ0yVsel1ddqkQgfLU5TvneYLmAX?usp=sharing

No Lake and Lake Model Analyses:
https://colab.research.google.com/drive/1iEb5ks6bg1A4bZzsQGE8Eq64rp4S4TGz?usp=sharing

Sensitivity Analyses:
https://colab.research.google.com/drive/1yBBnPquuIivbLVt5HC8dHbzhD1Az4_IF?usp=sharing

Field Work:
https://colab.research.google.com/drive/1Jop7v3dnopPp7g8uvq3cbO21XVGzGd6M?usp=sharing

Budgets:
https://colab.research.google.com/drive/11BzBHznRVmxOH3vAj5jPCLtEvgVFjIYq?usp=sharing